



HOKKAIDO UNIVERSITY

Title	Accumulation of humic-like fluorescent dissolved organic matter in the Japan Sea
Author(s)	Tanaka, Kazuki; Kuma, Kenshi; Hamasaki, Koji et al.
Citation	Scientific Reports, 4, 5292 https://doi.org/10.1038/srep05292
Issue Date	2014-07-16
Doc URL	https://hdl.handle.net/2115/56849
Rights(URL)	https://creativecommons.org/licenses/by/4.0/
Type	journal article
File Information	srep05292.pdf





OPEN

Accumulation of humic-like fluorescent dissolved organic matter in the Japan Sea

SUBJECT AREAS:
MARINE CHEMISTRY
BIOGEOCHEMISTRYKazuki Tanaka¹, Kenshi Kuma², Koji Hamasaki³ & Youhei Yamashita^{1,4}Received
26 March 2014Accepted
27 May 2014Published
16 July 2014Correspondence and
requests for materials
should be addressed to
Y.Y. (yamashiy@ees.
hokudai.ac.jp)¹Graduate School of Environmental Science, Hokkaido University, ²Faculty of Fisheries Science, Hokkaido University, ³Atmosphere and Ocean Research Institute, The University of Tokyo, ⁴Faculty of Environmental Earth Science, Hokkaido University.

Major fraction of marine dissolved organic matter (DOM) is biologically recalcitrant, however, the accumulation mechanism of recalcitrant DOM has not been fully understood. Here, we examine the distributions of humic-like fluorescent DOM, factions of recalcitrant DOM, and the level of apparent oxygen utilization in the Japan Sea. We find linear relationships between these parameters for the deep water (>200 m) of the Japan Sea, suggesting that fluorescent DOM is produced in situ in the Japan Sea. Furthermore, we find that the amount of fluorescent DOM at a given apparent oxygen utilization is greater in the deep water of the Japan Sea than it is in the North Pacific, where the highest level of fluorescent DOM in the open ocean was previously observed. We conclude that the repeated renewal of the deep water contributes to the accumulation of fluorescent DOM in the interior of the Japan Sea.

At 662 Pg C, oceanic dissolved organic matter (DOM) is a huge pool of reduced carbon, holding greater than 200 times the carbon inventory of marine biomass¹. The majority of oceanic DOM is considered to be of marine origin, and the microbial production of DOM (defined as the microbial carbon pump) has been implicated as one of the processes that produce recalcitrant DOM^{2,3}. Thus, it can be hypothesized that microbially derived, recalcitrant DOM accumulates in oceans. It has been hypothesized that oceanic DOM pool has been historically dynamic and that the changes in its size and the associated sequestration of CO₂ (at least 1600 PgC) or release of CO₂ from its degradation have affected the state of paleoclimates⁴. However, because the annual to decadal variation in the amount of recalcitrant DOM in oceans may be too small to detect, we do not know whether the present oceanic DOM pool is stable or dynamic⁵.

Though dissolved organic carbon (DOC) analyses can detect relatively small differences in DOM quantity due to recent improvements in analytical capabilities^{1,6}, DOC concentrations alone do not provide insights into the composition of DOM, which is useful for evaluating DOM dynamics^{6–9}. One of the more sensitive analytical methods for detecting DOM composition is the fluorescence technique^{10–12}. Though this technique can only evaluate fluorescent fractions in DOM, two major types of fluorophores, i.e., protein-like fluorophores (FDOM_A) and humic-like fluorophores (FDOM_H), can be detected using excitation-emission matrix (EEM) fluorescence^{10–14}. It is well documented that a major source of FDOM_H in coastal environments is the riverine inputs of terrestrial FDOM_H¹¹. Conversely, FDOM_H can also be produced during the microbial degradation of organic matter^{15–17}. Although FDOM_H is known to be easily degraded by sunlight^{18–20}, linear relationships between the fluorescence intensity of FDOM_H and indicators of microbial remineralization, namely, the apparent oxygen utilization (AOU), have been observed throughout deep oceans globally^{7,21–25}. In addition, the linear relationships between the amounts of FDOM_H and AOU present in the bathypelagic layer throughout the Pacific indicate that in situ-produced FDOM_H is bio-recalcitrant over the time scale of global thermohaline circulation (at least 900 years)⁷. These experimental and observational results suggest that FDOM_H is a product of the microbial carbon pump and is thus a useful indicator for evaluating DOM dynamics, especially its recalcitrant fraction.

The Japan Sea is a marginal sea in the western North Pacific that is connected to the East China Sea, the western North Pacific, and the Okhotsk Sea, and it has sills that are shallower than 150 m (Fig. 1). The Japan Sea spans from subarctic to subtropical conditions and is affected by global oceanic processes, e.g., subduction and deep-water formation. There is a relatively uniform water mass at the depths below thermocline that is named the Japan Sea Proper Water (JSPW)^{26–28}. The JSPW is known to contain high levels of oxygen and ¹⁴C of total dissolved inorganic carbon compared with other locations in the North Pacific and even the South Pacific, which is an indication of active deep convection^{28–32}. Due to its semi-closed characteristics, the turnover time of the JSPW by convection and the residence time of the water within the Japan Sea have been considered separately and are estimated to be 100 and 1000 years, respectively²⁹. The dissolved oxygen concentrations in the bottom layer of the JSPW have decreased during recent decades, indicating a weakening of the deep convection systems³¹.

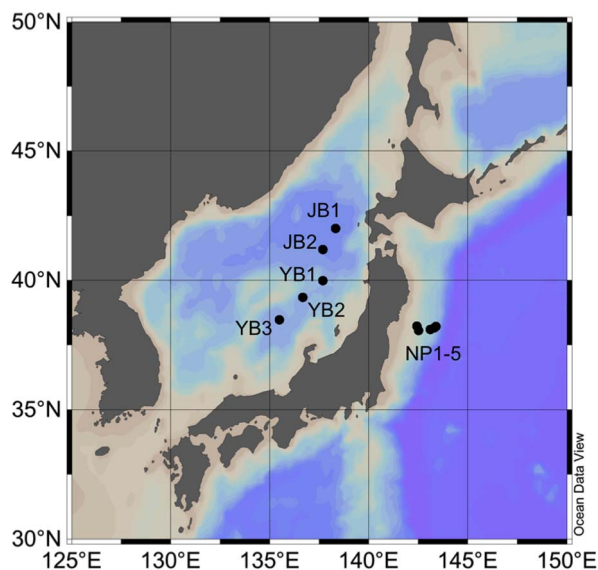


Figure 1 | Map of locations sampled for the survey of the FDOM_{H} distribution in the Japan Basin (JB1-2) and the Yamato Basin (YB1-3) of the Japan Sea and the western North Pacific (NP1-5). Map was created using Ocean Data View.

Though only a few studies have clarified the distributional patterns of DOM in the Japan Sea, it was reported that DOC concentrations in the JSPW were higher than those in deep waters of the North Pacific³³. Such high levels of DOC are possibly due to transport of semi-labile DOC from surface layers¹ along with the JSPW formation. On the other hand, similar levels of FDOM_{H} between the JSPW and the deep waters of the North Pacific were also reported³⁴. DOM in the deep waters of the North Pacific can be characterized as lowest DOC concentration^{1,5} and highest levels of recalcitrant FDOM_{H} ^{7,24} in the global deep ocean, indicative of the oldest DOM in the global ocean. Thus, there should be some specific mechanisms for keeping high levels of FDOM_{H} in the JSPW that age are significantly younger than the deep waters of the North Pacific³².

To obtain new insights into DOM dynamics in the JSPW as well as in the global ocean, we determined the spatial distributions of FDOM_{H} in the JSPW and in the deep waters of the western North Pacific (Fig. 1), two areas in which the levels of AOU differ significantly (Fig. 2). Water samples were collected from five sites in the Japan Sea (two in the Japan Basin and the others in the Yamato Basin) and five sites in the western North Pacific (Fig. 1). To evaluate the FDOM_{H} composition, filtered seawater samples were analyzed using EEM fluorescence and parallel factor analysis (PARAFAC)^{14,35}.

Results

FDOM_{H} in the Japan Sea. A three-component model was validated based on the PARAFAC modeling of EEMs from the Japan Sea and the western North Pacific (Fig. 3). Components 1 ($\text{FDOM}_{\text{H-1}}$) and 2

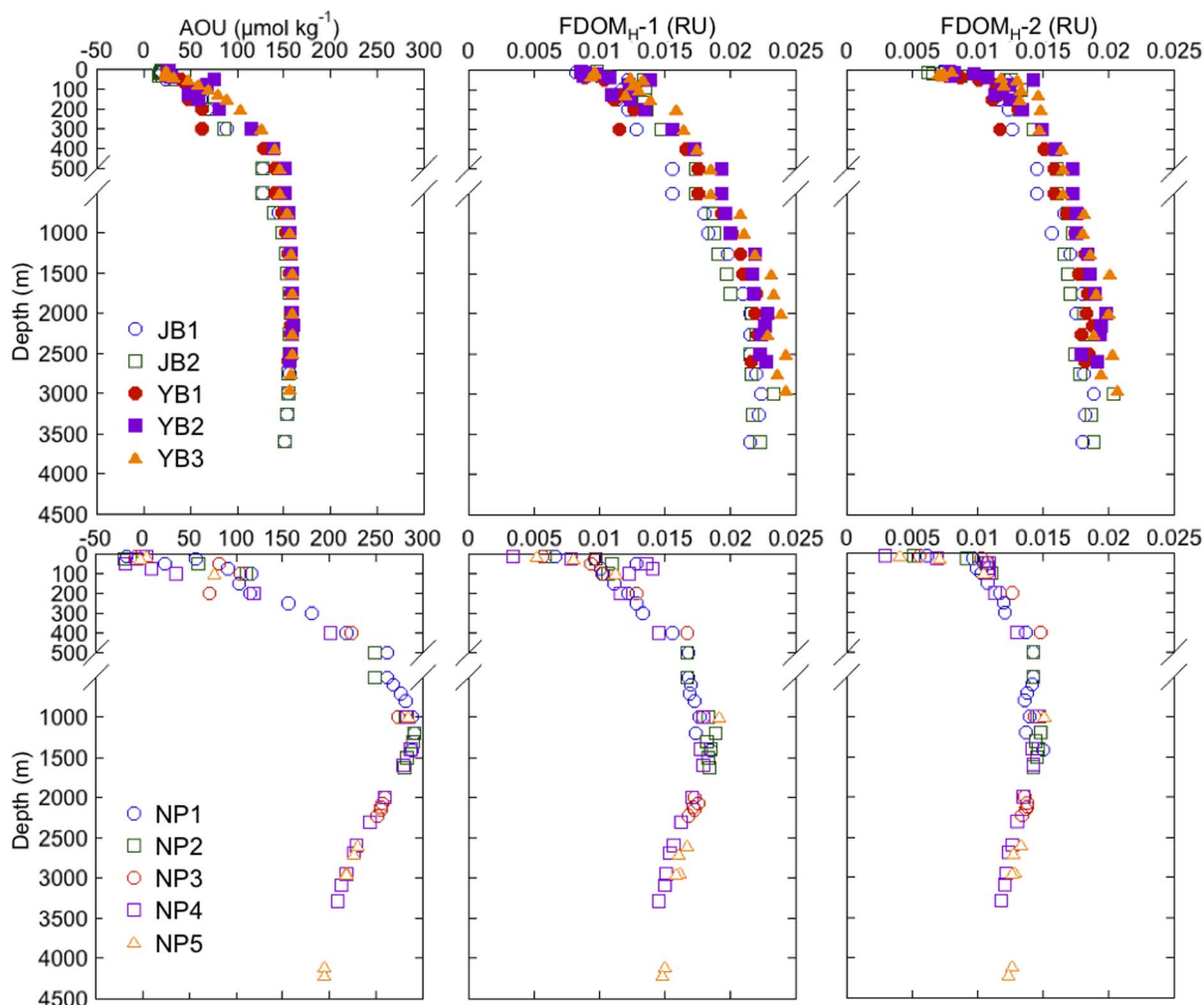


Figure 2 | Vertical profiles of AOU, $\text{FDOM}_{\text{H-1}}$, and $\text{FDOM}_{\text{H-2}}$ in the Japan Sea (upper panels) and the western North Pacific (lower panels).

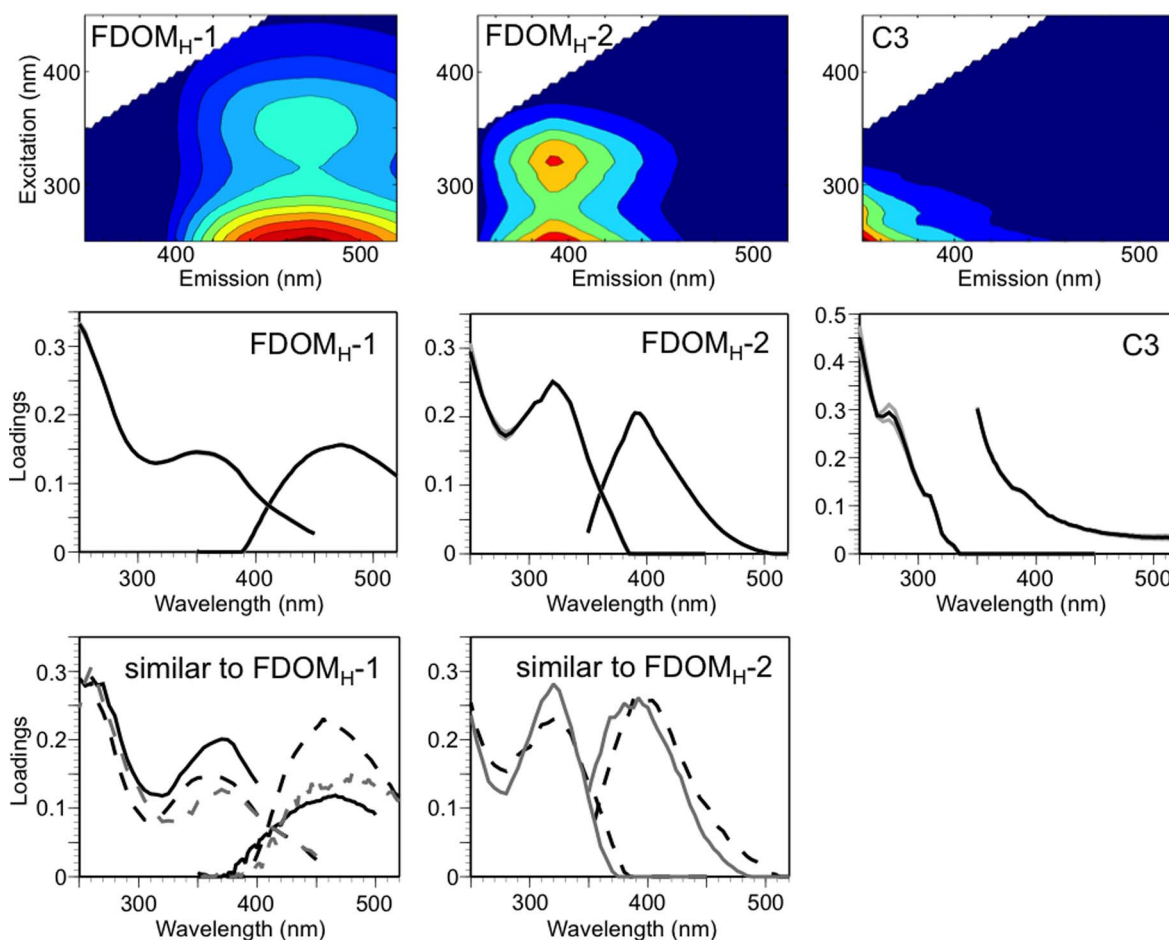


Figure 3 | Excitation emission matrix (upper panels) and validation (middle panels) of the three-component model by PARAFAC, and previously published similar PARAFAC components (lower panels). The grey lines in validation plots represent the results from the split half validation analysis. A black solid line, black broken line, grey solid line, and grey broken line in previously published PARAFAC components is from Ref. (23), Ref. (36), Ref. (24), and Ref. (37), respectively.

($FDOM_{H-2}$) exhibited fluorescence peaks in the region of humic-like fluorophores^{10–14}. Component 3 (C3) had a peak with an excitation wavelength less than 300 nm and an emission wavelength less than 350 nm and was characterized as representing protein-like fluorophores^{10–14}. Because we found a contamination peak that was similar to that of the protein-like fluorophores, C3 was considered to include the edge of the contamination peak and was thus not included in further analyses.

$FDOM_{H-1}$ had a peak at the 470-nm emission wavelength and could be categorized as a humic-like fluorophore that is traditionally defined as terrestrial^{10,11}. In contrast, $FDOM_{H-2}$ could be assigned as a humic-like fluorophore that is traditionally defined as marine because this $FDOM_H$ had a peak at the 395-nm emission wavelength^{10,11}. Similar PARAFAC components to $FDOM_{H-1}$ and $FDOM_{H-2}$ have been reported in previous EEM-PARAFAC studies that examined the open ocean^{23,24,36,37} (Fig. 3).

The vertical profiles of $FDOM_{H-1}$ and $FDOM_{H-2}$ were similar to each other in the Japan Sea, and this similarity was observed regardless of the sampling site examined (Fig. 2). The levels of $FDOM_H$ were the lowest in surface waters, gradually increased with depth, and were relatively constant at depths greater than 2000 m (Fig. 2). Though EEM-PARAFAC was firstly applied for the JSPW in the present study, similar vertical distributions of $FDOM_H$ were previously observed in the Japan Sea by measuring the fluorescence intensities at a single pair of excitation (320 nm) and emission (420 nm) wavelengths^{34,38} and by using EEM³³. In the western North Pacific, the amounts of $FDOM_{H-1}$ and $FDOM_{H-2}$ were also

lowest in the surface waters, followed by an increase with depth that peaked at 1000–1500 m and then decreased slightly with depth (Fig. 2). The vertical distribution of $FDOM_H$ in the western North Pacific was similar to those previously observed in the North Pacific^{7,23}. Though the highest levels of $FDOM_H$ previously observed in the open ocean globally were recorded for the intermediate water of the North Pacific^{7,24}, the amount of $FDOM_{H-1}$ and $FDOM_{H-2}$ measured in the JSPW was similar or slightly higher than that recorded in the intermediate water of the western North Pacific (Fig. 2). The vertical profiles of both $FDOM_H$ were similar with those of AOU for the Japan Sea and the western North Pacific (Fig. 2).

Relationships between $FDOM_H$ and AOU. The JSPW was divided into upper and deeper waters at 1000 m based on the vertical structure of potential temperature^{26,27}. Furthermore, the deeper JSPW can also be divided into two water masses at a depth of about 2000–2500 m^{26,28,32}. According to these criteria, the deep water masses in the Japan Sea were divided and defined as follows: the upper JSPW (UJSPW, 200–1000 m), the Japan Sea Deep Water (JSDW, 1000–2000 m), and the Japan Sea Bottom Water (JSBW, 2000 m–bottom). The deep water masses of the western North Pacific were separated into intermediate water (200–1000 m) and North Pacific Deep Water (NPDW, 1000 m–bottom) according to Refs. (7, 23). Except in the JSBW which contained a very narrow range of AOU and $FDOM_H$ values (Fig. 2), the $FDOM_{H-1}$ and $FDOM_{H-2}$ values were linearly correlated with the amount of AOU for the individual water masses of the Japan Sea and the

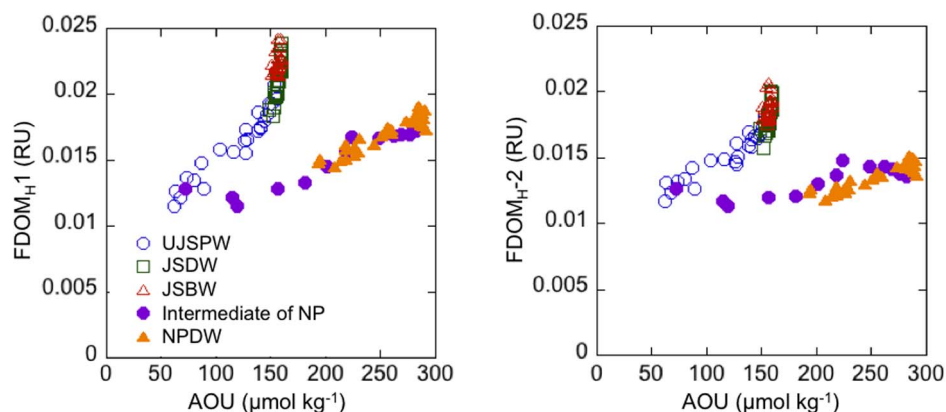


Figure 4 | FDOM_{H-1} and FDOM_{H-2} versus AOU in individual water masses of the ocean interior.

western North Pacific at depths below 200 m, where the photo-bleaching of FDOM_H can be negligible (Fig. 4; Table 1). The relationships between FDOM_H and AOU differed between the Japan Sea and the western North Pacific. Notably, the amount of FDOM_H at a given level of AOU was considerably greater for the Japan Sea compared with the western North Pacific.

Discussion

Similar to other oceans^{7,21–25}, we find linear relationships between AOU and FDOM_H for the deep water (>200 m) of the Japan Sea (Fig. 4; Table 1), indicating that both the FDOM_{H-1} (traditionally defined as terrestrial humic-like DOM) and the FDOM_{H-2} (traditionally defined as marine humic-like DOM) are produced in situ in the JSPW as organic matter is oxidized biologically. This result is similar to previous findings obtained for the open ocean^{23,24}. Interestingly, the relationships between FDOM_H and AOU differed between the Japan Sea and the western North Pacific, namely, the levels of FDOM_{H-1} and FDOM_{H-2} at a given AOU are greater for the Japan Sea compared with the western North Pacific. A possible cause for this difference in the FDOM_H-AOU relationships is a difference in the production mechanism of FDOM_H in the ocean interior, i.e., a difference in the ratio of FDOM_H production to oxygen consumption. However, a single linear regression between FDOM_H and AOU could be fit to the data for the bathypelagic layer throughout the Pacific⁷. In addition, one general linear regression fit the relationship between the amount of the fluorescent DOM components (corresponding to FDOM_{H-1} and FDOM_{H-2}) and the level of AOU for the global deep ocean²⁴. These previous findings imply that the characteristics of the production mechanism of FDOM_H are very similar, regardless of differences in oceanic regions. On the other hand, recent long-term (>1year) experiments revealed that production of FDOM_H depends on the lability of the substrate; the larger the production of FDOM_H relative to oxygen consumption was found for the less labile substrate¹⁵. The chemical composition of sinking

particles suggests that sinking particles at the deep layer is less labile compared with those at the intermediate layer³⁹, thus, differences in FDOM_H production against lability of sinking particles might be reason of differences in FDOM_H-AOU relationships among the UJSPW, JSDW, and JSBW (Fig. 4). Therefore, the difference between the FDOM_H-AOU relationships of the Japan Sea and the western North Pacific is possibly attributed to other factors and not to a difference in the production mechanism of FDOM_H, even though the difference found among the JSPW might be due to different lability of sinking particles.

Although a general FDOM_H-AOU linear relationship has been observed for the global ocean, the levels of FDOM_H found in the North Atlantic Deep Water (NADW) were relatively high compared with those expected based on the FDOM_H-AOU relationship for the global ocean²⁴. These deviations for the NADW have been attributed to the contribution of terrestrial FDOM_H derived from the Arctic Ocean because relatively high concentrations of lignin phenols, a unique terrestrial biomarker, were observed in the NADW⁴⁰. In the case of the Japan Sea, the Tsushima Warmer Current, which carries freshwater from the East China Sea, affects the surface water chemistry⁴¹. Terrestrial DOM derived from the Yangtze River, in particular, has been known to distribute into the East China Sea^{42,43}. In addition, freshwater from the Amur River has been known to flow into the northern part of the Japan Sea⁴⁴. Thus, in addition to in situ-produced FDOM_H, terrestrial DOM derived from the East China Sea and/or the Amur River might contribute to the surface water FDOM_H of the Japan Sea and thus to the JSPW.

In coastal environments, the shift of the peak position of FDOM_H to a shorter wavelength (blueshift) with an increase in salinity has been well documented^{10,11,45}. Such changes in emission maxima have been considered a result of the shift in the major fluorescent component from a terrestrial (corresponding to FDOM_{H-1}) to a marine origin (corresponding to FDOM_{H-2})^{45,46}. In other words, though both FDOM_{H-1} and FDOM_{H-2} are produced at oceanic as well as

Table 1 | Relationships between FDOM_H and AOU

	FDOM _{H-1} vs AOU				FDOM _{H-2} vs AOU			
	slope	intercept	R ²	n	slope	intercept	R ²	n
UJSPW	7.9×10^{-5}	0.0071	0.92	23	5.3×10^{-5}	0.0089	0.89	23
JSDW	44×10^{-5}	-0.047	0.73	25	28×10^{-5}	-0.026	0.55	25
JSBW		p > 0.05		24		p > 0.05		24
IW of NP	2.9×10^{-5}	0.0091	0.87	13	1.3×10^{-5}	0.011	0.62	13
NPDW	3.9×10^{-5}	0.007	0.88	32	2.7×10^{-5}	0.0066	0.85	32

The water masses are defined as follows: UJSPW = upper Japan Sea Proper Water (200–1000 m of the Japan Sea), JSDW = Japan Sea Deep Water (1000–2000 m of the Japan Sea), JSBW = Japan Sea Bottom Water (2000 m-bottom of the Japan Sea), IW of NP = intermediate water (200–1000 m) of the western North Pacific, and NPDW = North Pacific Deep Water (1000 m–bottom of the western North Pacific).

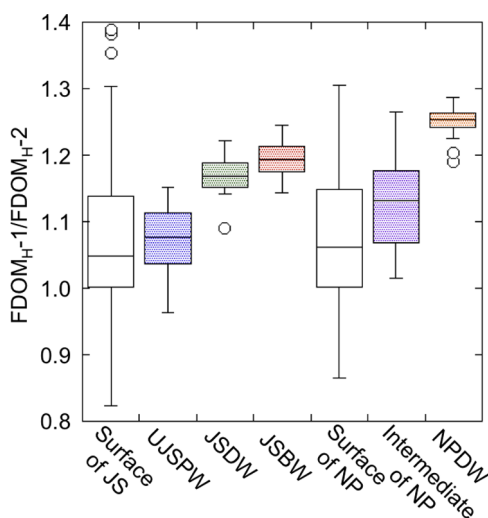


Figure 5 | The ratio of $FDOM_{H-1}$ to $FDOM_{H-2}$ for individual water masses. The boxes indicate the interquartile range (25th to 75th percentiles) and include the median value (midline); the whiskers indicate the 10th and 90th percentiles, and the symbols indicate the outliers. Surface of JS and surface of NP means surface waters (<200 m) of the Japan Sea and of the western North Pacific, respectively.

terrestrial environments, oceanic and terrestrial FDOM is rich in $FDOM_{H-2}$ and $FDOM_{H-1}$, respectively. In case of the JSPW, a higher contribution of terrestrial $FDOM_H$ would change the composition of the $FDOM_H$ by increasing the ratio of $FDOM_{H-1}$ to $FDOM_{H-2}$. However, the ratio of $FDOM_{H-1}$ to $FDOM_{H-2}$ in the JSPW was similar to or even lower than that in the intermediate and deep waters of the western North Pacific (Fig. 5), suggesting that the contribution of terrestrial $FDOM_H$ to the bulk $FDOM_H$ signature in the JSPW is similar to or smaller than that in the western North Pacific. The ratio of $FDOM_{H-1}$ to $FDOM_{H-2}$ tended to increase with depth (Fig. 5). A blueshift associated with photobleaching has been observed for both coastal and oceanic $FDOM_H$ ^{18,19}, suggesting that the $FDOM_H$ in shallower water masses is more photobleached compared with that found in deeper water masses and that the contribution of photobleached $FDOM_H$ in the JSPW is potentially greater than that in the western North Pacific. Although the vertical patterns of $FDOM_H$ composition cannot refute the possibility of the contribution of photobleached terrestrial $FDOM_H$ to the JSPW, the $FDOM_H$ -AOU linear relationship (Fig. 4) and conservative behavior of terrestrial chromophoric DOM including $FDOM_H$ in the Yangtze River estuary^{42,47} as well as the East China Sea⁴³ indicate that the contribution of photobleached terrestrial $FDOM_H$ is minor in the JSPW. The ratios measured in surface waters of the Japan Sea and the western North Pacific had large variations, suggesting that the contributions of terrestrial $FDOM_H$ and/or autochthonously produced $FDOM_H$ (and the corresponding organisms, including the marine phytoplankton¹⁶) in surface waters are different from those of the deep ocean.

Based on our findings and discussion above, the difference in the $FDOM_H$ -AOU relationships between the Japan Sea and the western North Pacific is potentially due to the process rather than the in situ production mechanism or the contribution of terrestrial $FDOM_H$. The JSPW is formed in the Japan Sea and has an independent convection system. During the deep convection process (the formation of the JSPW), original JSPW, which is characterized by high levels of AOU and $FDOM_H$ compared with surface waters, is transported to the surface layer; then, the level of the AOU decreases because of the mixing of JSPW with surface water and the supply of oxygen from the atmosphere. At the same time, the level of $FDOM_H$ also decreases with mixing but is not extensively degraded by photobleaching

because of the low winter insolation and the short residence time in the surface layer. It should be emphasized that the turnover time of the JSPW by convection is approximately 100 years, but its residence time within the Japan Sea is approximately 1000 years²⁹, indicating that most of the water that is upwelled by deep convection returns to the deep layer within a relatively short time scale and does not flow out of the Japan Sea into the North Pacific or the Okhotsk Sea. Hence, the water mass, which is characterized by a relatively low AOU and a relatively high $FDOM_H$, is subsequently redistributed as “new” JSPW. Thus, the in situ production of $FDOM_H$ in the JSPW and the repeated renewal of the JSPW result in the accumulation of $FDOM_H$ in the deep layer of the Japan Sea.

Although the amount of carbon in $FDOM_H$ has not been clearly determined, $FDOM_H$ may contribute to the high levels of DOC in the JSPW³³. The present study elucidates a potential mechanism for the accumulation of $FDOM_H$ in the deep ocean. Because $FDOM_H$ is bio-recalcitrant on a time scale similar to that of thermohaline circulation⁷ and the $FDOM_H$ pool in the open ocean is basically balanced by the rates of in situ production and photobleaching (and possibly contributions of terrestrial $FDOM_H$), the results of the present study indicate that $FDOM_H$ can accumulate in the ocean interior if this balance is upset by changes in processes such as the thermohaline circulation.

Methods

Samples from the Japan Sea were collected at 2 stations (JB1, JB2) in the Japan Basin and 3 stations (YB1, YB2, YB3) in the Yamato Basin from November 5 to 9, 2007, as part of the T/S *Oshoro-maru* cruise (C184). Water samples from the western North Pacific were collected at 5 stations from July 30 to August 3, 2011 as part of the R/V *Tansei Maru* cruise (KT-11-17). Salinity and temperature were measured using a CTD, and dissolved oxygen concentrations were measured using an oxygen sensor (SBE 43) connected to a CTD. Seawater samples for fluorescence analyses were collected with Niskin bottles. An in-line filter that was attached directly to the spigot of a Niskin bottle was used for filtration, and the seawater was gravity filtered. Acid-washed 0.22- μ m filters (Millipak 100 cartridge, Millipore) and pre-combusted glass fiber filters (GF/F, Whatman) were used to filter the Japan Sea and the western North Pacific samples, respectively. Thus, $FDOM_H$ levels in the Japan Sea may be slightly underestimated compared with those in the western North Pacific. Filtered samples were poured into 10-ml acrylic tubes and 20-ml pre-combusted glass ampoules for the Japan Sea and the western North Pacific, respectively, and were then stored frozen in the dark until analysis. The samples of the Japan Sea were collected in duplicate. The detailed results of the bulk fluorescence intensity at a 320-nm excitation and 420-nm emission, the dissolved and total dissolvable Fe concentrations, and the hydrographic parameters for the 5 stations in the Japan Sea have been reported previously³⁸.

Excitation-emission matrix (EEM) fluorescence spectra were obtained using a Horiba Fluoromax-4 fluorometer according to Ref. (48). Samples were thawed and allowed to stand until reaching near room temperature before the EEM measurement. Any residual particles were not observed when samples were thawed to room temperature. Forty-one emission scans from 290 to 550 nm taken at 2-nm intervals were acquired for the excitation wavelengths between 250 and 450 nm at 5-nm intervals. The bandpass was set to 5 nm for both excitation and emission. The fluorescence spectra were scanned with a 0.25-s integration time and acquired in the S/R mode. Several post-acquisition steps were involved in the correction of the fluorescence spectra, including instrumental bias correction and the subtraction of the EEM of Milli-Q water, and the fluorescence units were converted to Raman Units (RU)⁴⁹. The PARAFAC modeling was conducted in MATLAB (Mathworks, Natick, MA) using the DOMFluor toolbox³⁵. Contamination from protein-like fluorophores, possibly derived from the acrylic tubes, was evident for samples from the Japan Sea. Thus, the ranges of 250–450 nm and 350–520 nm for excitation and emission, respectively (excluding the wavelength range of the protein-like fluorophore contamination), were used for the PARAFAC modeling. The validation of the PARAFAC model was conducted according to Ref. (35). The spectra of two PARAFAC components, i.e., $FDOM_{H-1}$ and $FDOM_{H-2}$, were compared with those reported in earlier studies through online repository of published PARAFAC components⁵⁰ (Fig. 3). The similarity of components was statistically identified as having Tucker congruence exceeding 0.95. As a result, $FDOM_{H-1}$ was similar to C1 of Ref. (23), C4 of Ref. (36), and C2 of Ref. (37), and $FDOM_{H-2}$ was similar to C4 of Ref. (24) and C6 of Ref. (36). The average of $FDOM_{H-1}$ and $FDOM_{H-2}$ was reported for duplicate sample of the Japan Sea. The difference in fluorescence intensity was 0.0008 ± 0.0007 ($n = 112$) and 0.0010 ± 0.0008 ($n = 112$) for $FDOM_{H-1}$ and $FDOM_{H-2}$, respectively.

To evaluate any possible effect of contamination, $FDOM_{H-1}$ and $FDOM_{H-2}$, seawater samples were collected from the JSBW (2300–2730 m) at two stations during the T/S *Oshoro-maru* cruise (C253) conducted in April 2013. Seawater samples were collected using Niskin bottles and poured directly into pre-combusted glass vials with teflon-lined caps after triple rinsing to remove any possible contamination from tubes and filters. These samples were stored frozen in the dark until fluorescence



analyses. The EEMs of these samples did not show any contamination peaks in the region of the protein-like fluorophores. The fluorescence intensities of FDOM_{H-1} and FDOM_{H-2}, and FDOM_{H-1}/FDOM_{H-2} ranged from 0.0236–0.0241, 0.0192–0.0197, and 1.22–1.24 ($n = 10$), respectively. These values are within the same range observed for the JSBW at other stations (0.0215–0.0243, 0.0175–0.0207, and 1.14–1.24 for FDOM_{H-1}, FDOM_{H-2}, and FDOM_{H-1}/FDOM_{H-2}, respectively; Figs. 2 and 5), indicating that any contamination that possibly derived from the acrylic tubes did not affect the FDOM_H results.

- Hansell, D. A., Carlson, C. A., Repeta, D. J. & Shlitzer, R. Dissolved organic matter in the ocean: A controversy stimulates new insight. *Oceanogr.* **22**, 202–211 (2009).
- Ogawa, H., Amagai, Y., Koike, I., Kaiser, K. & Benner, R. Production of refractory dissolved organic matter by bacteria. *Science* **292**, 917–920 (2001).
- Jiao, N. *et al.* Microbial production of recalcitrant dissolved organic matter: long-term carbon storage in the global ocean. *Nat. Rev. Microbiol.* **8**, 593–599 (2010).
- Sexton, P. F. *et al.* Eocene global warming events driven by ventilation of oceanic dissolved organic carbon. *Nature* **471**, 349–352 (2011).
- Hansell, D. A. Recalcitrant dissolved organic carbon fractions. *Annu. Rev. Mar. Sci.* **5**, 421–445 (2013).
- Ogawa, H. & Tanoue, E. Dissolved organic matter in oceanic waters. *J. Oceanogr.* **59**, 129–147 (2003).
- Yamashita, Y. & Tanoue, E. Production of bio-refractory fluorescent dissolved organic matter in the ocean interior. *Nat. Geosci.* **1**, 579–582 (2008).
- Kaiser, K. & Benner, R. Biochemical composition and size distribution of organic matter at the Pacific and Atlantic time-series stations. *Mar. Chem.* **113**, 63–77 (2009).
- Dittmar, T. & Paeng, J. A heat-induced molecular signature in marine dissolved organic matter. *Nat. Geosci.* **2**, 175–179 (2009).
- Coble, P. G. Characterization of marine and terrestrial DOM in seawater using excitation-emission matrix spectroscopy. *Mar. Chem.* **51**, 325–346 (1996).
- Coble, P. G. Marine optical biogeochemistry: The chemistry of ocean color. *Chem. Rev.* **107**, 402–418 (2007).
- Mladenov, N. *et al.* Dust inputs and bacteria influence dissolved organic matter in clear alpine lakes. *Nat. Commun.* **2**, 405 (2011).
- Yamashita, Y. & Tanoue, E. Chemical characterization of protein-like fluorophores in DOM in relation to aromatic amino acids. *Mar. Chem.* **82**, 255–270 (2003).
- Stedmon, C. A., Markager, S. & Bro, R. Tracing dissolved organic matter in aquatic environments using a new approach to fluorescence spectroscopy. *Mar. Chem.* **82**, 239–254 (2003).
- Jørgensen, L., Stedmon, C. A., Granskog, M. A. & Middelboe, M. Tracing the long-term microbial production of recalcitrant fluorescent dissolved organic matter in seawater. *Geophys. Res. Lett.* **41**, 3481–2488 (2014).
- Romera-Castillo, C., Sarmento, H., Álvarez-Salgado, X. A., Gasol, J. M. & Marraés, C. Production of chromophoric dissolved organic matter by marine phytoplankton. *Limnol. Oceanogr.* **55**, 446–454 (2010).
- Shimotori, K., Watanabe, K. & Hama, T. Fluorescence characteristics of humic-like fluorescent dissolved organic matter produced by various taxa of marine bacteria. *Aquat. Microb. Ecol.* **65**, 249–260 (2012).
- Helms, J. R. *et al.* Photochemical bleaching of oceanic dissolved organic matter and its effect on absorption spectral slope and fluorescence. *Mar. Chem.* **155**, 81–91 (2013).
- Moran, M. A., Sheldon, Jr., W. M. & Zepp, R. G. Carbon loss and optical property changes during long-term photochemical and biological degradation of estuarine dissolved organic matter. *Limnol. Oceanogr.* **45**, 1254–1264 (2000).
- Omori, Y., Hama, T., Ishii, M. & Saito, S. Vertical change in the composition of marine humic-like fluorescent dissolved organic matter in the subtropical western North Pacific and its relation to photoreactivity. *Mar. Chem.* **124**, 38–47 (2011).
- Hayase, K. & Shinozuka, N. Vertical distribution of fluorescent organic matter along with AOU and nutrients in the equatorial Central Pacific. *Mar. Chem.* **48**, 283–290 (1995).
- Yamashita, Y., Tsukasaki, A., Nishida, T. & Tanoue, E. Vertical and horizontal distribution of fluorescent dissolved organic matter in the Southern Ocean. *Mar. Chem.* **106**, 498–509 (2007).
- Yamashita, Y. *et al.* Fluorescence characteristics of dissolved organic matter in the deep waters of the Okhotsk Sea and the northwestern North Pacific Ocean. *Deep-Sea Res. Part II* **57**, 1478–1485 (2010).
- Jørgensen, L. *et al.* Global trends in the fluorescence characteristics and distribution of marine dissolved organic matter. *Mar. Chem.* **126**, 139–148 (2011).
- Álvarez-Salgado, X. A. *et al.* New insights on the mineralization of dissolved organic matter in central, intermediate, and deep water masses of the northeast North Atlantic. *Limnol. Oceanogr.* **58**, 681–696 (2013).
- Nitani, H. in *Researches in Hydrography and Oceanography* (ed Shoji, D.) 151–201 (Hydrographical Department of Japan, Tokyo, 1972).
- Sudo, H. A note on the Japan Sea Proper Water. *Prog. Oceanogr.* **17**, 313–336 (1986).
- Gamo, T. & Horibe, Y. Abyssal circulation in the Japan Sea. *J. Oceanogr.* **39**, 220–230 (1983).
- Watanabe, Y. W., Watanabe, S. & Tsunogai, S. Tritium in the Japan Sea and the renewal time of the Japan Sea deep water. *Mar. Chem.* **34**, 97–108 (1991).
- Gamo, T., Momoshima, N. & Tolmachev, S. Recent upward shift of the deep convection system in the Japan Sea, as inferred from the geochemical tracers tritium, oxygen, and nutrients. *Geophys. Res. Lett.* **28**, 4143–4146 (2001).
- Gamo, T. Dissolved oxygen in the bottom water of the Sea of Japan as a sensitive alarm for global climate change. *Trac-Trends Anal. Chem.* **30**, 1308–1318 (2011).
- Kumamoto *et al.* Temporal and Spatial Variations of Radiocarbon in Japan Sea Bottom Water. *J. Oceanogr.* **64**, 429–441.
- Yamaguchi, Y., Nakaguchi, Y., Hattori, H., Kimura, M. & Hiraki, K. Anomalous distribution of dissolved organic carbon in the Sea of Japan. *Geochem. J.* **35**, 355–364 (2001).
- Takata, H. *et al.* Comparative vertical distributions of iron in the Japan Sea, the Bering Sea, and the western North Pacific Ocean. *J. Geophys. Res.* **110**, C07004 (2005).
- Stedmon, C. A. & Bro, R. Characterizing dissolved organic matter fluorescence with parallel factor analysis: a tutorial. *Limnol. Oceanogr. Meth.* **6**, 572–579 (2008).
- Stedmon, C. A., Thomas, D. N., Papadimitriou, S., Granskog, M. A. & Dieckmann, D. S. Using fluorescence to characterize dissolved organic matter in Antarctic sea ice brines. *J. Geophys. Res.* **116**, G03027 (2011).
- Kowalczyk, P. *et al.* Characterization of dissolved organic matter fluorescence in the South Atlantic Bight with use of PARAFAC model: Interannual variability. *Mar. Chem.* **113**, 182–196 (2013).
- Fujita, S. *et al.* Iron distributions in the water column of the Japan Basin and Yamato Basin (Japan Sea). *J. Geophys. Res.* **115**, C12001 (2010).
- Wakeham, S. G., Lee, C., Hedges, J. I., Hernes, P. J. & Peterson, M. L. Molecular indicators of diagenetic status in marine organic matter. *Geochim. Cosmochim. Acta* **61**, 5363–5369 (1997).
- Hernes, P. J. & Benner, R. Terrigenous organic matter sources and reactivity in the North Atlantic Ocean and a comparison to the Arctic and Pacific oceans. *Mar. Chem.* **100**, 66–79 (2006).
- Isobe, A. *et al.* Freshwater and temperature transports through the Tsushima-Korea Straits. *J. Geophys. Res.* **107**, C7, 3065. (2002).
- Guo, W. *et al.* The conservative and non-conservative behavior of chromophoric dissolved organic matter in Chinese estuarine waters. *Mar. Chem.* **107**, 357–366 (2007).
- Sasaki *et al.* Mapping the low salinity Changjiang Diluted Water using satellite retrieved colored dissolved organic matter (CDOM) in the East China Sea during high river flow season. *Geophys. Res. Lett.* **35**, L04604 (2008).
- Martin, S., Munoz, E. & Drucker, R. The effect of severe storms on the ice cover of the northern Tatarskiy Strait. *J. Geophys. Res.* **97**, C11, 17753–17764 (1992).
- Del Castillo, C. E., Gilbes, F., Coble, P. G. & Müller-Karger, F. E. On the dispersal of riverine colored dissolved organic matter over the West Florida Shelf. *Limnol. Oceanogr.* **45**, 1425–1432 (2000).
- Murphy, K. M., Stedmon, C. A., Waite, T. D. & Ruiz, G. M. Distinguishing between terrestrial and autochthonous organic matter sources in marine environments using fluorescence spectroscopy. *Mar. Chem.* **108**, 40–58 (2008).
- Sun, Q., Wang, C., Wang, P., Hou, J. & Ao, Y. Absorption and fluorescence characteristics of chromophoric dissolved organic matter in the Yangtze Estuary. *Environ. Sci. Pollut. Res.* **21**, 3460–3473 (2014).
- Yamashita, Y., Pantou, A., Mahaffey, C. & Jaffé, R. Assessing the spatial and temporal variability of dissolved organic matter in Liverpool Bay using excitation-emission matrix fluorescence and parallel factor analysis. *Ocean Dyn.* **61**, 569–579 (2011).
- Lawaetz, A. J. & Stedmon, C. A. Fluorescence intensity calibration using Raman scatter peak of water. *Appl. Spectrosc.* **63**, 936–940 (2009).
- Murphy, K. R., Stedmon, C. A., Wenig, P. & Bro, R. OpenFluor – an online spectral library of auto-fluorescence by organic compounds in the environment. *Anal. Methods* **6**, 658–661 (2014).

Acknowledgments

We thank Dr. T. Nagata and the captains and crews of the T/S *Oshoro-maru* and the R/V *Tansei Maru* for their assistance during observations. This study was supported by Grants-in-Aid for Scientific Research from Japan Society for the Promotion of Science (Nos. 24681002, 24121003).

Author contributions

Y.Y. contributed to the project planning, with discussion with K.K.; K.K. and K.H. planned the cruises and performed the sampling; K.T. and Y.Y. measured the samples, analyzed the data, and wrote the first draft of the manuscript; all authors contributed to the preparation of the final draft of the manuscript.

Additional information

Competing financial interests: The authors declare no competing financial interests.

How to cite this article: Tanaka, K., Kuma, K., Hamasaki, K. & Yamashita, Y. Accumulation of humic-like fluorescent dissolved organic matter in the Japan Sea. *Sci. Rep.* **4**, 5292; DOI:10.1038/srep05292 (2014).



This work is licensed under a Creative Commons Attribution 4.0 International License. The images or other third party material in this article are included in the article's Creative Commons license, unless indicated otherwise in the credit line; if

the material is not included under the Creative Commons license, users will need to obtain permission from the license holder in order to reproduce the material. To view a copy of this license, visit <http://creativecommons.org/licenses/by/4.0/>